ResearchGate

See discussions, stats, and author profiles for this publication at: https://www.researchgate.net/publication/291356970

Chimeric Mouse Model to Track the Migration of Bone Marrow Derived Cells in Glioblastoma Following Anti-angiogenic…

Article *in* Cancer biology & therapy · January 2016

DOI: 10.1080/15384047.2016.1139243

CITATIONS
3

READS
51

7 authors, including:

B.R Achyut
Augusta University
39 PUBLICATIONS **422** CITATIONS
SEE PROFILE

Adarsh Shankar
Augusta University
26 PUBLICATIONS **129** CITATIONS
SEE PROFILE

Robert Knight
Henry Ford Hospital
118 PUBLICATIONS **4,045** CITATIONS
SEE PROFILE

Ali S Arbab
Augusta University
202 PUBLICATIONS **6,255** CITATIONS
SEE PROFILE

Some of the authors of this publication are also working on these related projects:

Antiangiogenic therapy and vascular mimicry View project

All content following this page was uploaded by Ali S Arbab on 22 January 2016.

The user has requested enhancement of the downloaded file. All in-text references underlined in blue are added to the original document and are linked to publications on ResearchGate, letting you access and read them immediately.

cancer biology & therapy
Volume 16 - Issue 10 - October 2015

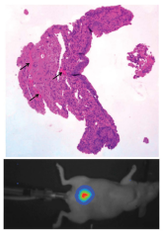

Taylor & Francis
Taylor & Francis Group

Cancer Biology & Therapy

ISSN: 1538-4047 (Print) 1555-8576 (Online) Journal homepage: http://www.tandfonline.com/loi/kcbt20

Chimeric Mouse Model to Track the Migration of Bone Marrow Derived Cells in Glioblastoma Following Anti-angiogenic Treatments

B.R. Achyut, Adarsh Shankar, A S M Iskander, Roxan Ara, Robert A. Knight, Alfonso G Scicli & Ali S. Arbab

To cite this article: B.R. Achyut, Adarsh Shankar, A S M Iskander, Roxan Ara, Robert A. Knight, Alfonso G Scicli & Ali S. Arbab (2016): Chimeric Mouse Model to Track the Migration of Bone Marrow Derived Cells in Glioblastoma Following Anti-angiogenic Treatments, Cancer Biology & Therapy, DOI: 10.1080/15384047.2016.1139243

To link to this article: http://dx.doi.org/10.1080/15384047.2016.1139243

View supplementary material

Accepted author version posted online: 21 Jan 2016.

Submit your article to this journal

View related articles

View Crossmark data

Full Terms & Conditions of access and use can be found at
http://www.tandfonline.com/action/journalInformation?journalCode=kcbt20

Download by: [Georgia Regents University Greenblatt Library] **Date:** 22 January 2016, At: 07:07

Downloaded by [Georgia Regents University Greenblatt Library] at 07:07 22 January 2016

Chimeric Mouse Model to Track the Migration of Bone Marrow Derived Cells in Glioblastoma Following Anti-angiogenic Treatments

B.R. Achyut[1], Adarsh Shankar[1], ASM Iskander[1], Roxan Ara[1], Robert A. Knight[2], Alfonso G Scicli[3], Ali S. Arbab[1,*]

[1]Tumor Angiogenesis Laboratory, Biochemistry and molecular biology, Cancer Center, Georgia Regents University, Augusta, GA

[2]NMR Center, Henry Ford Health System, Detroit, MI

[3]Cellular and Molecular Imaging Laboratory, Henry Ford Health System, Detroit, MI

[*]CORRESPONDING AUTHOR: Ali S Arbab, MD, PhD Tumor Angiogenesis Lab, Cancer Center, Georgia Regents University 1410 Laney Walker Blvd, CN3141, Augusta, GA 30912, USA Tel: 706-721-8909, Fax: 706-434-6406, Email:aarbab@gru.edu

Accepted manuscript

ABSTARCT

Bone marrow derived cells (BMDCs) have been shown to contribute in the tumor development. *In vivo* animal models to investigate the role of BMDCs in tumor development are poorly explored. We established a novel chimeric mouse model using as low as $5x10^6$ GFP+ BM cells in athymic nude mice, which resulted in >70% engraftment within 14 days. In addition, chimera was established in NOD-SCID mice, which displayed >70% with in 28 days. Since anti-angiogenic therapies (AAT) were used as an adjuvant against VEGF-VEGFR pathway to normalize blood vessels in glioblastoma (GBM), which resulted into marked hypoxia and recruited BMDCs to the tumor microenvironment (TME). We exploited chimeric mice in athymic nude background to develop orthotopic U251 tumor and tested receptor tyrosine kinase inhibitors and CXCR4 antagonist against GBM. We were able to track GFP+ BMDCs in the tumor brain using highly sensitive multispectral optical imaging instrument. Increased tumor

growth associated with the infiltration of GFP+ BMDCs acquiring suppressive myeloid and endothelial phenotypes was seen in TME following treatments. Immunofluorescence study showed GFP+ cells accumulated at the site of VEGF, SDF1 and PDGF expression, and at the periphery of the tumors following treatments. In conclusion, we developed a preclinical chimeric model of GBM and phenotypes of tumor infiltrated BMDCs were investigated in context of AATs. Chimeric mouse model could be used to study detailed cellular and molecular mechanisms of interaction of BMDCs and TME in cancer.

KEY WORDS

Glioblastoma, resistance, tumor angiogenesis, bone marrow, VEGF, microenvironment

Downloaded by [Georgia Regents University Greenblatt Library] at 07:07 22 January 2016

Accepted Manuscript

Downloaded by [Georgia Regents University Greenblatt Library] at 07:07 22 January 2016

INTRODUCTION

Glioblastoma (GBM), a grade IV glioma classified by World Health Organization (WHO), is considered highly malignant, vascular and invasive subtype.[1] GBM is most lethal during first year after initial diagnosis despite surgical resection, radiotherapy and/or chemotherapy [1, 2]. Hypoxia and neovascularization are histopathologic features of GBM [3]. Because of hypervascular nature of GBM, anti-angiogenic therapies (AAT) were used as an adjuvant mainly against VEGF-VEGFR pathway to normalize tumor vasculatures. Regrettably, benefits of antiangiogenic therapy are at best transitory, and this period of clinical benefit (measured in weeks or months) is followed by restoration of tumor growth and progression[4-7]. Agents that interfere with VEGF-VEGFR signal transduction pathway, such as vetanalib (PTK787), cediranib, sunitinib, etc have been used in clinical trials with varying degree of success[8, 9]. Evidence of relapse to progressive tumor growth following treatment reflects development of resistance to antiangiogenic therapies[10]. One possible mechanism for resistance to antiangiogenic therapy might be the activation of alternative angiogenesis signaling pathways, such as basic fibroblast growth factor (bFGF), Tie-2, stromal-cell derived factor-1α (SDF-1α), and increased VEGF production leading to increased invasiveness of the tumor cells[9, 11, 12]. A second additional and distinct potential mechanism of resistance might be recruitment of endothelial progenitor cells (EPCs) and pro-angiogenic monocytes from the bone marrow. Hypoxia creates conditions permissive for the recruitment of a heterogeneous population of bone marrow-derived monocytic cells that promotes angiogenesis and growth. However, animal models to *in vivo* track the migration and accumulation of BMDCs to the tumors are rare.

Current evidences from recent publications indicate the involvement of both angiogenesis and vasculogenesis processes for glioma growth (tumor growth)[13-15]. With an emerging new

Accepted Manuscript

insights into vasculogenesis, investigators are looking into possible mechanisms how bone marrow derived progenitor cells (BMPCs) or EPCs migrate and incorporate into tumor neovascularization[16]. One of the mechanisms, which has been pointed out is the involvement of SDF-1-CXCR4 axis [17-19]. SDF-1α is a chemokine that is expressed in tumor cells and released in the circulation following hypoxia in the tumor (with the up-regulation of HIF-1α) [20-22]. In an experiment, Heissig et al [23] determined the mechanisms of releasing hematopoietic stem cells (HSC) and EPCs from bone marrow. SDF-1α is a strong chemo-attractant for CXCR4 positive cells. Preventing interaction of SDF-1-CXCR4 is thought to be a mechanism to block vasculogenesis. AMD3100, a receptor (CXCR4) antagonist was initially developed as anti HIV drug and later used to mobilize CD34+ HSCs cells to the peripheral circulation [19]. Although AMD3100 increased the number of peripheral CD34+ or progenitor cells, the recent investigations pointed out that continuous treatment with AMD3100 or similar CXCR4 receptor antagonists inhibit vasculogenesis in tumors causing inhibition of tumor growth [19, 24]. *In vivo* determination of bone marrow cell mobilization and accumulation to tumor periphery and its effect in developing tumor resistance to antiangiogenic therapy would be invaluable[25].

Involvement of exogenously administered bone marrow or peripheral blood derived or endogenous bone marrow derived EPCs in tumor neovascularization has been determined mostly by invasive or ex vivo methods such as immunohistochemistry from biopsy materials or by fluorescent microscope following the administration of genetically altered EPCs. Alternatively investigators have used transgenic animal model (usually carrying reporter protein, such as green fluorescent (GFP) or red fluorescent protein (RFP)) to determine the involvement of endogenous cells in tumor neovascularization [26]. Two types of models have been used; 1) animals carrying reporter protein positive cells (such as GFP+), which is universally present in all cells of the

Downloaded by [Georgia Regents University Greenblatt Library] at 07:07 22 January 2016

Accepted Manuscript

Downloaded by [Georgia Regents University Greenblatt Library] at 07:07 22 January 2016

animals, 2) animals carrying promoter driven GFP+ cells that can only be present in endothelial cells. The later model has been used to determine tumor angiogenesis [26, 27]. Animals with universally GFP+ cells can be used to monitor the migration and involvement of GFP+ cells in implanted tumors but cannot differentiate involvement of surrounding (sprouting and co-opting) cells from bone marrow cells. Making of animal model that will allow *in vivo* tracking the involvement of endogenous bone marrow derived cells (BMDCs) to tumor development and neovascularization is challenging. The following criteria should be present to make an ideal model; 1) the animal should have reporter (such as GFP or RFP) only in bone marrow cells if the target is to determine the effect of bone marrow cells, 2) all other tissues of the body except bone marrow cells should not have any reporter positive cells, 3) tumors or lesion should be produced with cells that should not have similar reporter gene or protein. However, to be able to track the migration of reporter positive endogenous bone marrow cells by *in vivo* imaging, the number of promoter driven reporter positive cells should be sufficient enough or all migrated bone marrow cells should be positive for the reporter. Optical imaging (such as fluorescent or bioluminescent) and nuclear medicine imaging can be utilized to track the reporter gene positive endogenous cells to the sites of tumor or other lesions [28, 29].

Here we report our capability in establishing chimeric animal model, where only bone marrow cells express GFP. Detection of accumulation of GFP+ BMDCs to the implanted human GBM U251 cells as well as patients derived xenograft (PDX) of GBM is possible by *in vivo* optical imaging during anti-angiogenic/anti-vasculogenic treatments. We also show the effects of the drugs on GBM growth and the differential expression of myeloid and endothelial cells' signatures in accumulated BMDCs. We believe that chimeric models and available imaging modalities represent huge potential in translational cancer studies.

Accepted Manuscript

Downloaded by [Georgia Regents University Greenblatt Library] at 07:07 22 January 2016

RESULTS

Establishing chimeric mouse model

Athymic nude mice (n=3, each group) were transplanted with $5x10^6$ BM cells from GFP+ mouse after whole body irradiation of sub-lethal dose (6Gy). Engraftment efficiency (GFP+) was determined at each week (Days 7 to 56) (**Fig 1A**). Engraftment efficiency for NOD-SCID chimera was determined at different time points (Days 14 and 28) **(Supplementary Fig 1A)**. Non-injected group (non-irradiated) were used as control for flow cytometry gating. Highest engraftment efficiency of 22.3 % was achieved using i.p. injection (n=3) on day 56 (middle panel). Surprisingly, i.v. injection (n=3) of $5x10^6$ mononuclear cells achieved >70% engraftment by day 14 and >80 % engraftment by day 56 (lower panel) (**Fig 1B**). We decided to use i.v. injection of $5x10^6$ BM cells and 14 days waiting to establish chimera for tumor studies. However, in NOD-SCID chimera, 50% of mice showed more than 70% engraftment achieved by day 14 and 76% of mice displayed 83-87 % engraftment by day 28 **(Supplementary Fig 1B)**.

Effect of treatments on tumor growth

Chimeric athymic nude mice were implanted orthotopically with U251 cells and treated with vehicle (n=17), vatalanib (n=10), AMD3100 (n=9), and nintedanib (n=3) from day 8-21. All animals underwent MRI on day 22 (**Fig 2A and 2B)**. We selected vatalanib as AAT agent because these drugs enhanced tumor growth and activated alternate pathways of neovascularization in GBM [30, 31]. Nintedanib was used to investigate the effect of multi-tyrosine kinase inhibition in GBM. In addition, AMD3100 is an immunostimulant used to mobilize bonemarrow derived hematopoietic stem cells in tumor. We observed no significant decrease in tumor growth after vatalanib and AMD3100 treatment. Nintedanib treatment resulted

Accepted Manuscript

in increased tumor growth as observed by MRI and tumor volume data **(Fig 2A and 2B**). NOD-SCID chimera (n=6) were orthotopically implanted with GBM PDX cells for tumor studies. However, we could not perform MRI with NOD-SCID chimera due to unexpected sickness. NOD-SCID mice were euthanized, whenever sign of sickness were seen.

Effect of treatments on infiltration of GFP+ cells in the tumor

In vivo optical images obtained on days 7, 14 and 21 showed more accumulation of GFP+ in tumor following treatments (yellow arrows) compared to vehicle (**Fig 3A and 3B**). Nintedanib and AMD3100 treatments showed increased accumulation of GFP+ cells in tumor at day 14 compared to vehicle group (yellow arrows). At day 21, optical images showed increased infiltration of GFP+ cells in vatalanib, nintedanib and AMD3100 treated groups compared to vehicle (yellow arrows). Similarly, flow cytometry data at the end of the study (day 22) proved higher number of GFP+ cells in drug treated tumors compared to vehicle, especially with nintedanib treatment (**Fig 3C**,). GBM PDX bearing NOD-SCID chimera were scanned on days 14 and 18, which showed accumulation of GFP+ in the tumor regions of the brain **(Supplementary Fig 2A and B)**. In addition, ex-vivo imaging following mice euthanasia showed accumulation of GFP+ in the tumor regions of the brain (**Supplementary Fig 2C)**.

Effect of vatalanib, nintedanib and AMD3100 on myeloid and endothelial cell signatures

Post-MRI, brain, spleen and BM were collected and processed for flowcytometry to analyze immune cell signatures (spleen and BM data not shown). Vatalanib treatment significantly increased both myeloid signature (CD68) and endothelial signatures (CD133, CD31, CD202b, CD34) compared to vehicle (**Fig 4A and 4B**). In addition, significant increase in endothelial cell

Downloaded by [Georgia Regents University Greenblatt Library] at 07:07 22 January 2016

Accepted Manuscript

signatures (CD133 and CD31) was seen in nintedanib group compared to vehicle (**Fig 4A and 4B**). Please note we did not performt CD68, CD202b and CD34 stainings in nintedanib group (**Fig 4A and 4B**). No significant changes in myeloid and endothelial cell signatures were seen in AMD3100 group (**Fig 4A and 4B**). In addition, rumor brains from NOD-SCID chimera bearing GBM PDX were collected on day 18 and processed for flow cytometry analysis. Tumor displayed 8% of bone marrow derived GFP+ cells**.** GFP+ cells polarized in to myeloid cell phenotypes such as Gr1+ CD11b+ (59.3%), F4/80+ CD11b+ (63.1%) and CD68+ CD11b+ (49.6%), and endothelial cell phenotypes such as CD202b (62.4%), CD309 (67.1%), CD34 (55.6%), CD133 (87.7%) and CD144 (16.7%), respectively (**Supplementary Fig 3A)**. High GFP positivity (99.8%) was seen in corresponding bone marrow populations. GFP+ cells in bone marrow displayed increased immature markers and decreased mature markers of myeloid cell phenotypes such as Gr1+ CD11b+ (93.5%), F4/80+ CD11b+ (17.4%) and CD68+ CD11b+ (6.01%), and endothelial cell phenotypes such as CD202b (83.2%), CD309 (33.6%), CD34 (76%), CD133 (87.3%) and CD144 (0.88%), respectively (**Supplementary Fig 3B)**.

Homing sites and phenotypes of infiltrated GFP+ cells

Immunofluorescence study showed accumulation of GFP+ cells at the tumor periphery or invasive front in vatalanib treated group (yellow arrow). Vehicle and other treatments showed more disperse GFP+ cell accumulation throughout the tumor (**Fig 5A**). Accumulation of GFP+ cells was seen at the site of PDGF, SDF1 and VEGF expression in the TME (**Fig 5B**). We checked whether the treaments have changed the phenotype of cells with myeloid signatures in the TME. Immunofluorescence study clearly showed increased GFP+ cells alongwith increased CD11b+ and F4/80+ cells in vatalanib, nintedanib and AMD3100 treated groups compared to

Downloaded by [Georgia Regents University Greenblatt Library] at 07:07 22 January 2016

Accepted Manuscript

vehicle (yellow arrows) (**Fig 5C**). However, we did not perform immunofluorescence study in NOD-SCID mice.

DISCUSSION

We established a novel chimeric mouse model with more than 70% engraftment efficiency in 2 weeks using $5x10^6$ GFP+ bone marrow cells. Our chimera mouse model in nude background is superior to previously published models, which needs 4 weeks to establish with same number of cells engrafted[32, 33]. Chimera in NOD-SCID background showed almost similar engraftment efficiency, implanted with human GBM PDX but could not survive longer for AATs. We noticed increased infiltration of GFP+ BMDCs in TME and increased tumor growth as shown by MRI data following vatalanib, nintedanib and CXCR4 antagonist (AMD 3100). Our observation corroborates with previous report where anti-VEGF recruited increased GFP+ BMDCs in TIB6, B16F1, EL4 and LLC tumor-bearing mice[33]. In our observation, GFP+ BMDCs were invaded throughout tumor but more concentrated at invasive front of tumor and overlapped with expression of VEGF, SDF1 and PDGF.

We used orthotopic mouse model with human glioma cells (U251) that better recapitulate histopathological feature of GBM compared to that of subcutaneous models due to differences in gene expression profile and TME [34, 35]. Previous studies that used U87 cell line, doesn't recapitulate human GBM completely compared to U251 [36]. As indicated in human GBMs, orthotopic mice models with U251 revealed similar level of expression of GFAP, S100B, and Vimentin markers [35] and deletion of p53, PTEN and INK4a/ARF at the genetic level [35, 37]. Intracranial U251 model demonstrated infiltrative invasion into brain parenchyma and significant foci of palisading necrosis microscopically. There are several other *in vivo* mice models exist to understand the biology of GBM [38]. In addition, few mouse models are available that can offer the

Downloaded by [Georgia Regents University Greenblatt Library] at 07:07 22 January 2016

Accepted Manuscript

in vivo tracking and study of tumor recruited BMDCs in development AAT resistance [32, 33]. However, role of tumor recruited BMDCs in GBM is poorly studied and no mouse model can offer early engraftment of GFP+ bone marrow compared to present mouse model.

Bone marrow cells have pivotal role in tumor development. CXCR4+ BMDCs are recruited to the tumor through up-regulation of HIF1-α followed by induction of SDF1α, secretion of pro-angiogenic factors [39-42]. These recruited cells were characterized as pro-angiogenic CD45+VEGFR2+ EPCs, or CD45+Tie2+ monocytes [43, 44]. BMDCs derived MMP9 modulated neovessels remodeling and contributing in tumor growth [42, 45]. Interestingly, lin-ckit+Sca-1+ and their derived cells demonstrated recruitment to tumor but do not functionally contribute to tumor neovascularization [46]. Since, AATs have been failed so far, therefore, tumor recruited BMDCs needed further investigation in context to therapeutic resistance.

Studies have indicated that resistance to AAT has profound involvement of immune system [47-53]. Role of myeloid cells in tumor angiogenesis is an established phenomenon as shown by previous studies [54-58] and supported by our current study. Vatalanib treatment significantly increased both myeloid signature (CD68) and endothelial signatures (CD133, CD31, CD202b, CD34). Majority of GFP+ cells acquire endothelial phenotype bearing CD133 and CD31 markers in nintedanib group.This differential effect of vatalanib and nintedanib could be due to difference in number of molecular targets e.g. nintedanib (VEGFR2, VEGFR3, LCK, FLT3, VEGFR1, FGFR2, PDGFRα, PDGFRβ, FGFR1, FGFR3, Src, Lyn, FGFR4, IGF1R, Insulin Receptor, CDK1, CDK2, CDK4, EGFR and HER2) and vatalanib (VEGFR2/KDR, VEGFR1/FLT1, VEGFR2/Flk1, PDGFRβ, VEGFR3/FLT4, c-Kit and c-Fms). Previous study showed similar findings, where SDF-1α played an important role in brain tumor invasion and macrophage infiltration in a murine astrocytoma [59], however, authors did not test any AAT. In

Downloaded by [Georgia Regents University Greenblatt Library] at 07:07 22 January 2016

Accepted Manuscript

other study, authors observed that AATs in U87 tumors were associated with increased myeloid cell infiltration and stem cell accumulation. However, investigations whether those phenotypes have bone marrow component are lacking [36]. Similar to our report, authors noticed that increased infiltration in myeloid populations in the tumor bulk and in the infiltrative regions after AAT [51]. Together, studies suggest that immune suppressive myeloid cells (especially MDSCs and TAM [60, 61]) may participate in escape from AATs, may represent a potential biomarker of resistance and a potential therapeutic target in GBM [51]. We also tested combined treatments of vatalanib and AMD3100; however, it did not decrease tumor growth (data not shown). Previously, combined treatment of murine and human VEGF specific antibody and CXCR4 antagonist, POL5551, significantly increased survival of mice bearing GBM [62]. We believe that use of different drugs could be the reason of this differential effect.

Several mechanisms have been known to regulate mobilization and recruitment immature myeloid cells into the TME, e.g. IL17 induced expression of GCSF through NF-κB and ERK signaling helped homing of myeloid cells to the tumor [47]. Bv8 modulated mobilization of MDSCs from BM to the tumor and promoted angiogenesis [54]. MDSCs can be produced in BM in response to tumor derived factors i.e. GCSF, IL6, GMCSF, IL1β, PGE2 and TNFα, and were recruited to tumor site by CXCL12 and CXCL5 [63]. TGFβ signaling in BMDCs is important and recruits MDSCs via CCL2 in TME [64]. CEACAM1 is identified as negative regulator of myeloid cell expansion and recruitment by inhibiting GCSF-Bv8 axis [55]. Similarly, TIMP2 was shown to down regulate expression of immunosuppressive genes controlling MDSC growth such as IL10, IL13, IL11 and chemokine ligand (CCL5/RANTES), and increased IFN-γ and decreased CD40L [65]. Recently, CXCL7 was discovered as an critical chemokine in myeloid cell associated

Downloaded by [Georgia Regents University Greenblatt Library] at 07:07 22 January 2016

Accepted Manuscript

cancer[66]. Our current chimeric mouse model could be used for future molecular mechanism studies of therapeutic resistance in glioma and other solid cancers.

In conclusion, we developed preclinical chimeric mouse models with earlier engraftment efficiency (2 weeks, >70%) compared to available models (4 weeks). We studied the contribution of tumor infiltrated BMDCs in AAT resistance in GBM. Clinical trials involving AATs have failed so far; therefore, our model may provide a tool to investigate altered myeloid cells and associated molecular networks in GBM. As shown by others before, our study supports that inhibiting key immune suppressive myeloid cells in TME could provide a better therapeutic option in GBM.

MATERIALS AND METHODS

All Animal related experimental procedures were approved by the Institutional Animal Care and Use Committee and Institutional Review Board of Georgia Regents University (animal protocol #2014-0625). All efforts were made to ameliorate suffering of animals. CO2 with secondary method was used to euthanize animals for tissue collection.

Establishing chimeric mouse model

Chimeric mouse for orthotopic U251 glioma was established with IACUC approved protocol and published method [67]. Transgenic mice with universally expressing GFP under the human ubiquitin C promoter (C57BL/6-tg(UBC-GFP)30Scha) were used as donors (Jackson Laboratory, Main, USA). NCr-nu/nu athymic nude (Charles River, Frederick, MD, USA) and NOD-SCID mice (Harlan laboratory, Indianapolis, USA) were used as recipients, and were whole body irradiated with sub-lethal dose of 6Gy (Cs137). After 24 hours, recipient athymic nude mice were injected intravenous (IV) (n=3) and intraperitoneal (n=3) routes with BM cells

Downloaded by [Georgia Regents University Greenblatt Library] at 07:07 22 January 2016

Accepted Manuscript

($5x10^6$ cells) collected from donor transgenic mice. NOD-SCID mice (n=6) were injected with BM cells ($5x10^6$ cells) through IV route.

Briefly, all mononuclear cells were separated from red blood cells using lymphocyte cell separation media (Corning, Cellgro, USA), counted and $5x10^6$ cells/100µl were injected into each mouse. Ten microliter of blood (from orbital sinus) were collected from each athymic mouse on days 7 to 56 (n=3 each time point) following transplantation of BM to determine BM engraftment efficiency (GFP positivity) in peripheral blood using flowcytometer. Engraftment efficiency of NOD-SCID mice was determined at different time points (Days 14 and 28) using flow cytometry. Cells from athymic mice without irradiation and GFP+ cell transplantation were used as control for flow cytometry. Our results showed that by 14 days all mice with IV administration of GFP+ bone marrow cells had effcicent bone marrow engraftment. However, 50% of mice showed more than 70% engraftment achieved by day 14 and 75% of mice displayed 83-87 % engraftment by day 28. Based on the optimal results, all subsequent chimeric animals were created using IV administration of GFP+ bone marrow cells and the orthotopic GBM implanted on day 15 in athymic chimera and day 29 in NOD-SCID chimera, following IV administration of GFP+ cells.

Animal model of human glioma

Following establishment of chimeric mice, animals were anesthetized with 100 mg/kg ketamine and 15 mg/kg xylazine i.p. The surgical zone was swabbed with betadine solution, the eyes coated with Lacri-lube and the animals were immobilized in a small animal stereotactic device (Kopf, Cayunga, CA). After draping, a 1-cm incision was made 2 mm to the right of the midline 1 mm retro-orbitally; the skull exposed with cotton-tip applicators and a 23G needle tip was used

Downloaded by [Georgia Regents University Greenblatt Library] at 07:07 22 January 2016

Accepted Manuscript

to drill a hole 2 mm to the right of the bregma, taking care not to penetrate the dura. A 10µL Hamilton syringe with a 26G-needle containing U251 tumor cells or GBM PDX ($n=2.4x10^5$) in 3 µl was lowered to a depth of 2.5 mm, and then raised to a depth of 2 mm. During and after the injection, careful note was made of any reflux from the injection site. After completing the injection, we waited 2-3 minutes before withdrawing in a stepwise manner. The surgical hole was sealed with bone wax. Finally, the skull was swabbed with betadine before suturing the skin over the injection site.

In vivo multispectral optical imaging

Multispectral optical images were acquired using excitation profiles of 460-480 nm range and emission of 510 to 570 nm to monitor the GFP color at days 7, 14 and 21 after tumor cell implantation. All optical imaging data was acquired by Kodak In-Vivo Multispectral Imaging System FX (Carestream) and analyzed by Carestream software. For NOD-SCID chimera, *In vivo* optical images obtained by Spectral AMI (Spectral Instruments Imaging, LLC) machines and analyzed by AMI view software. Based on signal intensities derived from different excitation and emission profiles, we have fixed our excitation and emission profile at 480 and 535, respectively, for all subsequent experiments.

Drug treatments

Orthotopically implanted chimeric mice with U251 tumor cells were allowed to grow for 7 days and then started oral treatments of either vehicle or receptor tyrosine kinase inhibitors (vatalanib (50mg/kg/day) [68] and nintadanib (50mg/kg/day) [69]), daily for two weeks. AMD3100 (10mg/kg/day) [70] treatment was given through ALZET osmotic pumps **(**DURECT Corporation,

Downloaded by [Georgia Regents University Greenblatt Library] at 07:07 22 January 2016

Accepted Manuscript

CA USA) for two weeks. Seven days waiting period was followed after tumor implantation to mimic clinical scenario, where treatment is being done following detection of tumor.

***In vivo* magnetic resonance imaging (MRI)**

To determine the tumor growth at the end of treatments, all animals underwent MRI on day 22. All MRI experiments were conducted using a 7 Tesla 12 cm (clear bore) magnet interfaced to a varian console with actively shielded gradients of 49 gauss/cm and 100μs rise times or a horizontal 7 Tesla BioSpec MRI spectrometer (Brucker Instruments, Bellerica, MA) equipped with a 12 cm self-shielded gradient set (45 gauss/cm max). Detailed MRI procedure was adopted from our several previous publications [71-75]. An appropriate state of anesthesia was obtained with isoflurane (2.5% for induction, 0.7% to 1.5% for maintenance in a 2:1 mixture of N_2:O_2). After positioning using a triplanar FLASH sequence, MR studies were performed using pre-contrast T1, T2-weighted and post contrast T1-weighted MRI scans with following parameters (1) Standard T1-weighted multislice sequence (TR/TE=500/10 ms, 256x256 matrix, 13-15 slices, 1 mm thick slice, 32 mm field of view (FOV), # of averages=4). (2) T2-mapping sequence (2D multi-slice, multi-echo (MSME) sequence, TE=10, 20, 30, 40, 50, 60 msec, TR=3000 msec, 256x256 matrix, 13-15 slices, 1 mm thick slice, 32 mm field of view (FOV), # of averages=2). Post contrast T1WI was used to determine volume of tumors in vehicle and drug treated mice by drawing irregular ROI to encircle whole tumor in each image section containing tumor using ImageJ software, and area was then multiplied by thickness of image slice to determine volume (cm^3). Two investigators blinded to the animal groups determined tumor volume.

Collection of GFP+ cells and determination of different cell populations

Downloaded by [Georgia Regents University Greenblatt Library] at 07:07 22 January 2016

Accepted Manuscript

Freshly isolated brain samples were separated into left and right (tumor bearing) hemispheres from each group and were homogenized to pass through 40µ cell strainer to make single cell. Similarly, cells were collected from spleen and BM. Cells were labeled with antibodies (BioLegend) such as CD45, Gr1, CD11b, F4/80, CD68, CD133, CD31, CD34, CD202b (Tie2), and CD309 (VEGFR2) (other than FITC) to identify BM recruited cell types (GFP+) in the tumor. Flow cytometry data was acquired using Accuri C6 machine (BD Biosciences) and analyzed by BD Accuri C6 software.

Immunofluorescence study

Frozen tissue sections were prepared using standard protocols and later stained for immunofluorescence study to determine expression of angiogenic markers such as VEGF (Santa Cruz Biotechnology), SDF-1α (Abcam) and PDGF (Santa Cruz Biotechnology) at the site of tumor. Migration and incorporation pattern of GFP+ BMDCs was determined in different regions of the tumor. Myeloid cell signature markers for example CD11b (Abcam) and F4/80 (Santa Cruz Biotechnology) were also determined.

Statistical analysis

Quantitative data was expressed as mean ± SD and analyzed through one way analysis of variance (ANOVA) followed by Fisher's least significant difference (FLSD) post-hoc test. Group to group analysis was performed using student t-test but analysis between nindtedanib and other groups was performed by non-parametric Mann Wintney test. Differences were considered statistically significant at p value <0.05.

Downloaded by [Georgia Regents University Greenblatt Library] at 07:07 22 January 2016

Accepted Manuscript

ACKNOWLEDGEMENT

Authors thank GRU cancer center small animal imaging core facility for finishing project on timely manner.

Downloaded by [Georgia Regents University Greenblatt Library] at 07:07 22 January 2016

Accepted Manuscript

Downloaded by [Georgia Regents University Greenblatt Library] at 07:07 22 January 2016

Accepted Manuscript

REFERENCES

1. Olar A, Aldape KD. Using the molecular classification of glioblastoma to inform personalized treatment. The Journal of pathology 2014; 232:165-77.

2. Stupp R, Mason WP, van den Bent MJ, Weller M, Fisher B, Taphoorn MJ, Belanger K, Brandes AA, Marosi C, Bogdahn U, et al. Radiotherapy plus concomitant and adjuvant temozolomide for glioblastoma. The New England journal of medicine 2005; 352:987-96.

3. Brat DJ, Van Meir EG. Vaso-occlusive and prothrombotic mechanisms associated with tumor hypoxia, necrosis, and accelerated growth in glioblastoma. Laboratory investigation; a journal of technical methods and pathology 2004; 84:397-405.

4. Miller KD, Sweeney CJ, Sledge GW, Jr. Can tumor angiogenesis be inhibited without resistance? EXS 2005:95-112.

5. Thompson EM, Frenkel EP, Neuwelt EA. The paradoxical effect of bevacizumab in the therapy of malignant gliomas. Neurology 2011; 76:87-93.

6. Grabner G, Nobauer I, Elandt K, Kronnerwetter C, Woehrer A, Marosi C, Prayer D, Trattnig S, Preusser M. Longitudinal brain imaging of five malignant glioma patients treated with bevacizumab using susceptibility-weighted magnetic resonance imaging at 7 T. Magn Reson Imaging 2012; 30:139-47.

7. Wong ET, Gautam S, Malchow C, Lun M, Pan E, Brem S. Bevacizumab for recurrent glioblastoma multiforme: a meta-analysis. J Natl Compr Canc Netw 2011; 9:403-7.

8. Norden AD, Drappatz J, Wen PY. Antiangiogenic therapy in malignant gliomas. Curr Opin Oncol 2008; 20:652-61.

9. Norden AD, Drappatz J, Wen PY. Novel anti-angiogenic therapies for malignant gliomas. Lancet Neurol 2008; 7:1152-60.

Downloaded by [Georgia Regents University Greenblatt Library] at 07:07 22 January 2016

10. Bergers G, Hanahan D. Modes of resistance to anti-angiogenic therapy. Nature Review Cancer 2008; 8:592-603.

11. Kerbel RS. Tumor angiogenesis. The New England journal of medicine 2008; 358:2039-49.

12. Batchelor TT, Sorensen AG, di Tomaso E, Zhang WT, Duda DG, Cohen KS, Kozak KR, Cahill DP, Chen PJ, Zhu M, et al. AZD2171, a pan-VEGF receptor tyrosine kinase inhibitor, normalizes tumor vasculature and alleviates edema in glioblastoma patients. Cancer cell 2007; 11:83-95.

13. Folkins C, Shaked Y, Man S, Tang T, Lee CR, Zhu Z, Hoffman RM, Kerbel RS. Glioma Tumor Stem-Like Cells Promote Tumor Angiogenesis and Vasculogenesis via Vascular Endothelial Growth Factor and Stromal-Derived Factor 1. Cancer Res 2009; 69:7243-51.

14. Dome B, Hendrix MJC, Paku S, Tovari J, Timar J. Alternative Vascularization Mechanisms in Cancer: Pathology and Therapeutic Implications. Am J Pathol 2007; 170:1-15.

15. Yu L, Su B, Hollomon M, Deng Y, Facchinetti V, Kleinerman ES. Vasculogenesis Driven by Bone Marrow-Derived Cells Is Essential for Growth of Ewing's Sarcomas. Cancer research 2010; 70:1334-43.

16. Patenaude A, Parker J, Karsan A. Involvement of endothelial progenitor cells in tumor vascularization. Microvascular Research 2010; 79:217-23.

17. Shichinohe H, Kuroda S, Yano S, Hida K, Iwasaki Y. Role of SDF-1/CXCR4 system in survival and migration of bone marrow stromal cells after transplantation into mice cerebral infarct. Brain research 2007; 1183:138-47.

18. Jin DK, Shido K, Kopp HG, Petit I, Shmelkov SV, Young LM, Hooper AT, Amano H, Avecilla ST, Heissig B, et al. Cytokine-mediated deployment of SDF-1 induces revascularization

Accepted Manuscript

through recruitment of CXCR4(+) hemangiocytes. Nat Med 2006; 12:557-67. Epub 2006 Apr 30.

19. Petit I, Jin D, Rafii S. The SDF-1-CXCR4 signaling pathway: a molecular hub modulating neo-angiogenesis. Trends in Immunology 2007; 28:299-307.

20. Ceradini DJ, Kulkarni AR, Callaghan MJ, Tepper OM, Bastidas N, Kleinman ME, Capla JM, Galiano RD, Levine JP, Gurtner GC. Progenitor cell trafficking is regulated by hypoxic gradients through HIF-1 induction of SDF-1. Nat Med 2004; 10:858-64. Epub 2004 Jul 4.

21. Arbab AS, Janic B, Knight RA, Anderson SA, Pawelczyk E, Rad AM, Read EJ, Pandit SD, Frank JA. Detection of migration of locally implanted AC133+ stem cells by cellular magnetic resonance imaging with histological findings. FASEB journal : official publication of the Federation of American Societies for Experimental Biology 2008; 22:3234-46.

22. Moore MA, Hattori K, Heissig B, Shieh JH, Dias S, Crystal RG, Rafii S. Mobilization of endothelial and hematopoietic stem and progenitor cells by adenovector-mediated elevation of serum levels of SDF-1, VEGF, and angiopoietin-1. Annals of the New York Academy of Sciences 2001; 938:36-45; discussion -7.

23. Heissig B, Hattori K, Dias S, Friedrich M, Ferris B, Hackett NR, Crystal RG, Besmer P, Lyden D, Moore MA, et al. Recruitment of stem and progenitor cells from the bone marrow niche requires MMP-9 mediated release of kit-ligand. Cell 2002; 109:625-37.

24. Kioi M, Vogel H, Schultz G, Hoffman RM, Harsh GR, Brown JM. Inhibition of vasculogenesis, but not angiogenesis, prevents the recurrence of glioblastoma after irradiation in mice. J Clin Invest 2010; 120:694-705.

25. Hentschel SJ, Sawaya R. Optimizing outcomes with maximal surgical resection of malignant gliomas. Cancer Control 2003; 10:109-14.

Downloaded by [Georgia Regents University Greenblatt Library] at 07:07 22 January 2016

Accepted Manuscript

26. Hillen F, Kaijzel EL, Castermans K, oude Egbrink MG, Lowik CW, Griffioen AW. A transgenic Tie2-GFP athymic mouse model; a tool for vascular biology in xenograft tumors. Biochem Biophys Res Commun 2008; 368:364-7.

27. Motoike T, Loughna S, Perens E, Roman BL, Liao W, Chau TC, Richardson CD, Kawate T, Kuno J, Weinstein BM, et al. Universal GFP reporter for the study of vascular development. Genesis 2000; 28:75-81.

28. Jang KS, Lee KS, Yang SH, Jeun SS. In vivo Tracking of Transplanted Bone Marrow-Derived Mesenchymal Stem Cells in a Murine Model of Stroke by Bioluminescence Imaging. J Korean Neurosurg Soc 2010; 48:391-8.

29. Ray P, Tsien R, Gambhir SS. Construction and validation of improved triple fusion reporter gene vectors for molecular imaging of living subjects. Cancer Res 2007; 67:3085-93.

30. Ali MM, Janic B, Babajani-Feremi A, Varma NR, Iskander AS, Anagli J, Arbab AS. Changes in vascular permeability and expression of different angiogenic factors following anti-angiogenic treatment in rat glioma. PloS one 2010; 5:e8727.

31. Arbab AS. Activation of alternative pathways of angiogenesis and involvement of stem cells following anti-angiogenesis treatment in glioma. Histology and histopathology 2012; 27:549-57.

32. Pyonteck SM, Akkari L, Schuhmacher AJ, Bowman RL, Sevenich L, Quail DF, Olson OC, Quick ML, Huse JT, Teijeiro V, et al. CSF-1R inhibition alters macrophage polarization and blocks glioma progression. Nature medicine 2013; 19:1264-72.

33. Shojaei F, Wu X, Malik AK, Zhong C, Baldwin ME, Schanz S, Fuh G, Gerber HP, Ferrara N. Tumor refractoriness to anti-VEGF treatment is mediated by CD11b+Gr1+ myeloid cells. Nature biotechnology 2007; 25:911-20.

Downloaded by [Georgia Regents University Greenblatt Library] at 07:07 22 January 2016

Accepted Manuscript

34. Camphausen K, Purow B, Sproull M, Scott T, Ozawa T, Deen DF, Tofilon PJ. Orthotopic growth of human glioma cells quantitatively and qualitatively influences radiation-induced changes in gene expression. Cancer research 2005; 65:10389-93.

35. Jacobs VL, Valdes PA, Hickey WF, De Leo JA. Current review of in vivo GBM rodent models: emphasis on the CNS-1 tumour model. ASN neuro 2011; 3:e00063.

36. Piao Y, Liang J, Holmes L, Zurita AJ, Henry V, Heymach JV, de Groot JF. Glioblastoma resistance to anti-VEGF therapy is associated with myeloid cell infiltration, stem cell accumulation, and a mesenchymal phenotype. Neuro-oncology 2012; 14:1379-92.

37. Radaelli E, Ceruti R, Patton V, Russo M, Degrassi A, Croci V, Caprera F, Stortini G, Scanziani E, Pesenti E, et al. Immunohistopathological and neuroimaging characterization of murine orthotopic xenograft models of glioblastoma multiforme recapitulating the most salient features of human disease. Histology and histopathology 2009; 24:879-91.

38. Simeonova I, Huillard E. In vivo models of brain tumors: roles of genetically engineered mouse models in understanding tumor biology and use in preclinical studies. Cellular and molecular life sciences : CMLS 2014; 71:4007-26.

39. Aghi M, Cohen KS, Klein RJ, Scadden DT, Chiocca EA. Tumor stromal-derived factor-1 recruits vascular progenitors to mitotic neovasculature, where microenvironment influences their differentiated phenotypes. Cancer research 2006; 66:9054-64.

40. De Falco E, Porcelli D, Torella AR, Straino S, Iachininoto MG, Orlandi A, Truffa S, Biglioli P, Napolitano M, Capogrossi MC, et al. SDF-1 involvement in endothelial phenotype and ischemia-induced recruitment of bone marrow progenitor cells. Blood 2004; 104:3472-82.

Downloaded by [Georgia Regents University Greenblatt Library] at 07:07 22 January 2016

Accepted Manuscript

41. Ceradini DJ, Kulkarni AR, Callaghan MJ, Tepper OM, Bastidas N, Kleinman ME, Capla JM, Galiano RD, Levine JP, Gurtner GC. Progenitor cell trafficking is regulated by hypoxic gradients through HIF-1 induction of SDF-1. Nature medicine 2004; 10:858-64.

42. Ahn GO, Brown JM. Matrix metalloproteinase-9 is required for tumor vasculogenesis but not for angiogenesis: role of bone marrow-derived myelomonocytic cells. Cancer cell 2008; 13:193-205.

43. Deak E, Gottig S, Ruster B, Paunescu V, Seifried E, Gille J, Henschler R. Bone marrow derived cells in the tumour microenvironment contain cells with primitive haematopoietic phenotype. Journal of cellular and molecular medicine 2010; 14:1946-52.

44. Ahn GO, Brown JM. Role of endothelial progenitors and other bone marrow-derived cells in the development of the tumor vasculature. Angiogenesis 2009; 12:159-64.

45. Seandel M, Butler J, Lyden D, Rafii S. A catalytic role for proangiogenic marrow-derived cells in tumor neovascularization. Cancer cell 2008; 13:181-3.

46. Shinde Patil VR, Friedrich EB, Wolley AE, Gerszten RE, Allport JR, Weissleder R. Bone marrow-derived lin(-)c-kit(+)Sca-1+ stem cells do not contribute to vasculogenesis in Lewis lung carcinoma. Neoplasia 2005; 7:234-40.

47. Chung AS, Wu X, Zhuang G, Ngu H, Kasman I, Zhang J, Vernes JM, Jiang Z, Meng YG, Peale FV, et al. An interleukin-17-mediated paracrine network promotes tumor resistance to anti-angiogenic therapy. Nature medicine 2013; 19:1114-23.

48. Shojaei F, Wu X, Qu X, Kowanetz M, Yu L, Tan M, Meng YG, Ferrara N. G-CSF-initiated myeloid cell mobilization and angiogenesis mediate tumor refractoriness to anti-VEGF therapy in mouse models. Proceedings of the National Academy of Sciences of the United States of America 2009; 106:6742-7.

Downloaded by [Georgia Regents University Greenblatt Library] at 07:07 22 January 2016

Accepted Manuscript

49. Seton-Rogers S. Tumour microenvironment: Means of resistance. Nature reviews Cancer 2013; 13:607.

50. Phan VT, Wu X, Cheng JH, Sheng RX, Chung AS, Zhuang G, Tran C, Song Q, Kowanetz M, Sambrone A, et al. Oncogenic RAS pathway activation promotes resistance to anti-VEGF therapy through G-CSF-induced neutrophil recruitment. Proceedings of the National Academy of Sciences of the United States of America 2013; 110:6079-84.

51. Lu-Emerson C, Snuderl M, Kirkpatrick ND, Goveia J, Davidson C, Huang Y, Riedemann L, Taylor J, Ivy P, Duda DG, et al. Increase in tumor-associated macrophages after antiangiogenic therapy is associated with poor survival among patients with recurrent glioblastoma. Neuro-oncology 2013; 15:1079-87.

52. Achyut BR. Impact of Microenvironment in Therapy-Induced Neovascularization of Glioblastoma. Biochem Physiol 2013; 2:e121.

53. Dondossola E, Rangel R, Guzman-Rojas L, Barbu EM, Hosoya H, St John LS, Molldrem JJ, Corti A, Sidman RL, Arap W, et al. CD13-positive bone marrow-derived myeloid cells promote angiogenesis, tumor growth, and metastasis. Proceedings of the National Academy of Sciences of the United States of America 2013; 110:20717-22.

54. Shojaei F, Wu X, Zhong C, Yu L, Liang XH, Yao J, Blanchard D, Bais C, Peale FV, van Bruggen N, et al. Bv8 regulates myeloid-cell-dependent tumour angiogenesis. Nature 2007; 450:825-31.

55. Lu R, Kujawski M, Pan H, Shively JE. Tumor angiogenesis mediated by myeloid cells is negatively regulated by CEACAM1. Cancer research 2012; 72:2239-50.

56. Shojaei F, Zhong C, Wu X, Yu L, Ferrara N. Role of myeloid cells in tumor angiogenesis and growth. Trends in cell biology 2008; 18:372-8.

Downloaded by [Georgia Regents University Greenblatt Library] at 07:07 22 January 2016

Accepted Manuscript

57. Yang L, DeBusk LM, Fukuda K, Fingleton B, Green-Jarvis B, Shyr Y, Matrisian LM, Carbone DP, Lin PC. Expansion of myeloid immune suppressor Gr+CD11b+ cells in tumor-bearing host directly promotes tumor angiogenesis. Cancer cell 2004; 6:409-21.

58. Achyut BR, Arbab, A.S. Myeloid Derived Suppressor Cells: Fuel the Fire. Biochem Physiol 2014; 3:e123.

59. Wang SC, Hong JH, Hsueh C, Chiang CS. Tumor-secreted SDF-1 promotes glioma invasiveness and TAM tropism toward hypoxia in a murine astrocytoma model. Laboratory investigation; a journal of technical methods and pathology 2012; 92:151-62.

60. Sica A, Schioppa T, Mantovani A, Allavena P. Tumour-associated macrophages are a distinct M2 polarised population promoting tumour progression: potential targets of anti-cancer therapy. European journal of cancer 2006; 42:717-27.

61. Hussain SF, Yang D, Suki D, Aldape K, Grimm E, Heimberger AB. The role of human glioma-infiltrating microglia/macrophages in mediating antitumor immune responses. Neuro-oncology 2006; 8:261-79.

62. Barone A, Sengupta R, Warrington NM, Smith E, Wen PY, Brekken RA, Romagnoli B, Douglas G, Chevalier E, Bauer MP, et al. Combined VEGF and CXCR4 antagonism targets the GBM stem cell population and synergistically improves survival in an intracranial mouse model of glioblastoma. Oncotarget 2014; 5:9811-22.

63. Sawanobori Y, Ueha S, Kurachi M, Shimaoka T, Talmadge JE, Abe J, Shono Y, Kitabatake M, Kakimi K, Mukaida N, et al. Chemokine-mediated rapid turnover of myeloid-derived suppressor cells in tumor-bearing mice. Blood 2008; 111:5457-66.

Downloaded by [Georgia Regents University Greenblatt Library] at 07:07 22 January 2016

Accepted Manuscript

64. Fan Q, Gu D, Liu H, Yang L, Zhang X, Yoder MC, Kaplan MH, Xie J. Defective TGF-beta signaling in bone marrow-derived cells prevents hedgehog-induced skin tumors. Cancer research 2014; 74:471-83.

65. Guedez L, Jensen-Taubman S, Bourboulia D, Kwityn CJ, Wei B, Caterina J, Stetler-Stevenson WG. TIMP-2 targets tumor-associated myeloid suppressor cells with effects in cancer immune dysfunction and angiogenesis. Journal of immunotherapy 2012; 35:502-12.

66. Achyut BR, Shankar A, Iskander A, Ara R, Angara K, Zeng P, Knight RA, Scicli AG, Arbab AS. Bone marrow derived myeloid cells orchestrate antiangiogenic resistance in glioblastoma through coordinated molecular networks. Cancer letters 2015.

67. Ali MM, Kumar S, Shankar A, Varma NR, Iskander AS, Janic B, Chwang WB, Jain R, Babajeni-Feremi A, Borin TF, et al. Effects of tyrosine kinase inhibitors and CXCR4 antagonist on tumor growth and angiogenesis in rat glioma model: MRI and protein analysis study. Translational oncology 2013; 6:660-9.

68. Yuen DA, Stead BE, Zhang Y, White KE, Kabir MG, Thai K, Advani SL, Connelly KA, Takano T, Zhu L, et al. eNOS deficiency predisposes podocytes to injury in diabetes. Journal of the American Society of Nephrology : JASN 2012; 23:1810-23.

69. Richeldi L, Costabel U, Selman M, Kim DS, Hansell DM, Nicholson AG, Brown KK, Flaherty KR, Noble PW, Raghu G, et al. Efficacy of a tyrosine kinase inhibitor in idiopathic pulmonary fibrosis. The New England journal of medicine 2011; 365:1079-87.

70. Yu M, Gang EJ, Parameswaran R, Stoddart S, Fei F, Schmidhuber S, Park E, Hsieh YT, Yang AS, Groffen J, et al. AMD3100 sensitizes acute lymphoblastic leukemia cells to chemotherapy in vivo. Blood cancer journal 2011; 1:e14.

Downloaded by [Georgia Regents University Greenblatt Library] at 07:07 22 January 2016

Accepted Manuscript

71. Ding G, Jiang Q, Zhang L, Zhang ZG, Li L, Knight RA, Ewing JR, Wang Y, Chopp M. Analysis of combined treatment of embolic stroke in rat with r-tPA and a GPIIb/IIIa inhibitor. Journal of Cerebral Blood Flow & Metabolism 2005; 25:87-97.

72. Conway JG, McDonald B, Parham J, Keith B, Rusnak DW, Shaw E, Jansen M, Lin PY, Payne A, Crosby RM, et al. Inhibition of colony-stimulating-factor-1 signaling in vivo with the orally bioavailable cFMS kinase inhibitor GW2580. Proceedings of the National Academy of Sciences of the United States of America 2005; 102:16078-83.

73. Ewing JR, Knight RA, Nagaraja TN, Yee JS, Nagesh V, Whitton PA, Li L, Fenstermacher JD. Patlak plots of Gd-DTPA MRI data yield blood-brain transfer constants concordant with those of 14C-sucrose in areas of blood-brain opening. Magn Reson Med 2003; 50:283-92.

74. Nagaraja TN, Karki K, Ewing JR, Divine GW, Fenstermacher JD, Patlak CS, Knight RA. The MRI-measured arterial input function resulting from a bolus injection of Gd-DTPA in a rat model of stroke slightly underestimates that of Gd-[14C]DTPA and marginally overestimates the blood-to-brain influx rate constant determined by Patlak plots. Magnetic Resonance in Medicine 2010; 63:1502-9.

75. Nagaraja TN, Karki K, Ewing JR, Croxen RL, Knight RA. Identification of Variations in Blood-Brain Barrier Opening After Cerebral Ischemia by Dual Contrast-Enhanced Magnetic Resonance Imaging and T1sat Measurements. Stroke 2008; 39:427-32.

Downloaded by [Georgia Regents University Greenblatt Library] at 07:07 22 January 2016

Accepted Manuscript

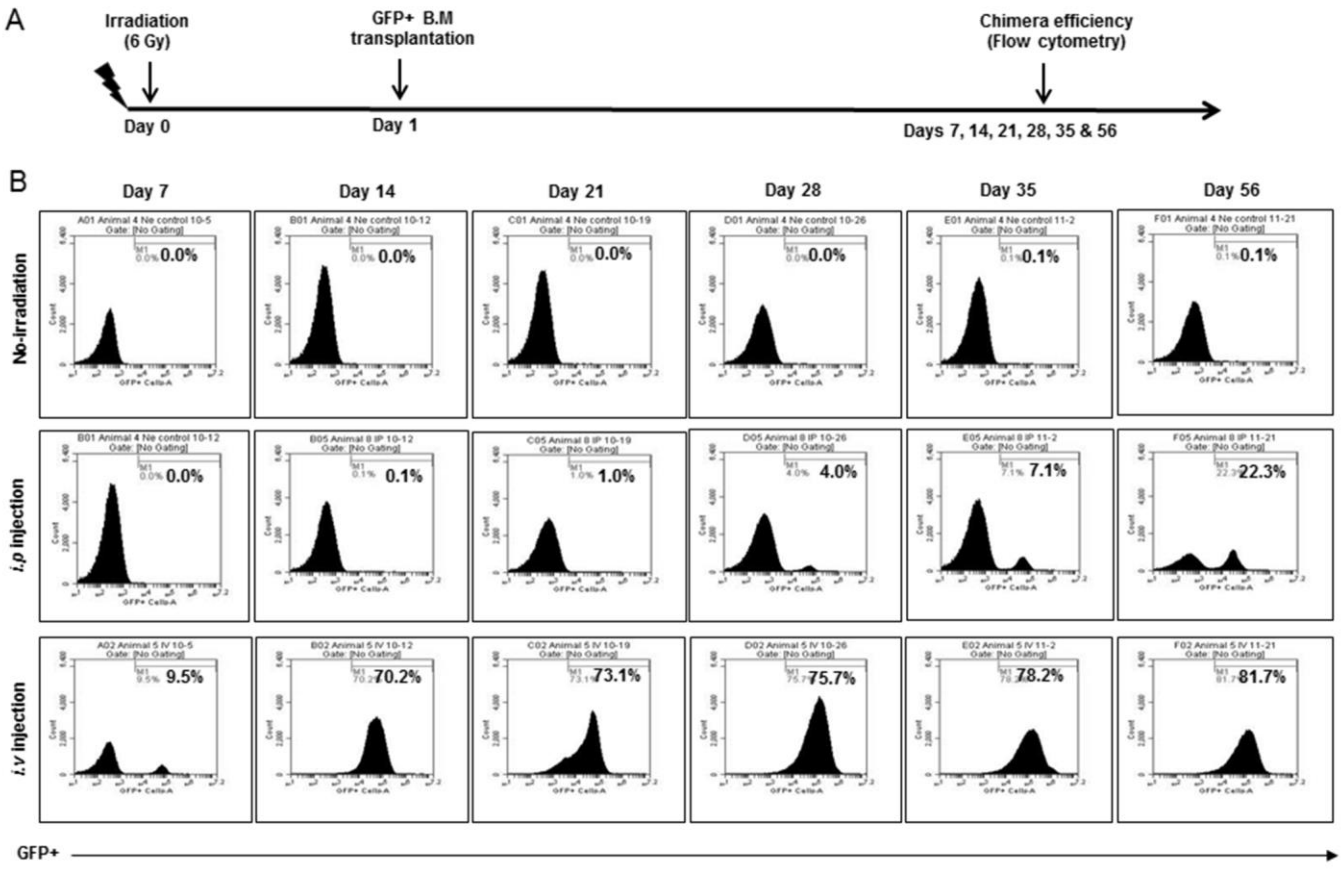

Figure 1. **Establishing chimeric mouse model:** (**A)** After whole body irradiation with sub-lethal dose (6Gy), athymic mice were transplanted with freshly isolated bone marrow cells from GFP+ mouse. Engraftment efficiency was determined at different time points (Days 7 to 56). (**B**) Non irradiation group (upper panel) was used as control for flow cytometry gating strategy. Highest engraftment efficiency of 22.3 % was achieved using i.p. route injection on day 56 (middle panel). However, >70% engraftment can be achieved by day 14 and >80 % engraftment by day 56 (lower panel) with i.v. injection of >5 million mononuclear cells.

Accepted

Downloaded by [Georgia Regents University Greenblatt Library] at 07:07 22 January 2016

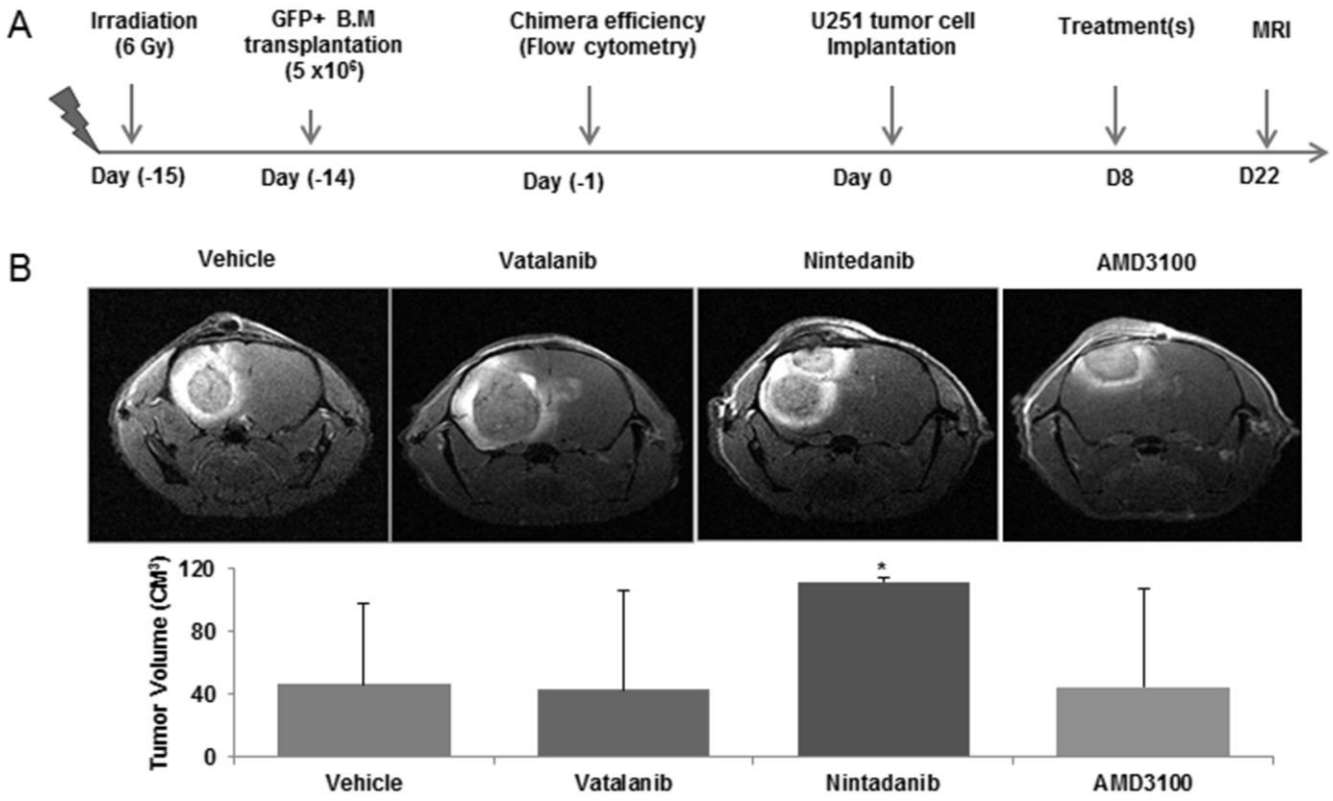

Figure 2. Effect of treatments on tumor growth: Chimeric animals were implanted with orthotopic glioma (U251) and treated with vehicle, vatalanib, nintedanib and AMD3100 from day 8-21. **(A)** Schematic of chimera establishment, U251 tumor cells implantation, drug treatments and *in vivo* MRI. (**B)** All animals underwent MRI on day 22 following implantation of tumors. No significant reduction in tumor growth was observed using vatalanib and AMD3100. Surprisingly, Nintedanib treatment resulted in increased tumor growth as observed by MRI and tumor volume data. Quantitative data is expressed in mean ±SD. *P<0.05.

Downloaded by [Georgia Regents University Greenblatt Library] at 07:07 22 January 2016

Accepted

Downloaded by [Georgia Regents University Greenblatt Library] at 07:07 22 January 2016

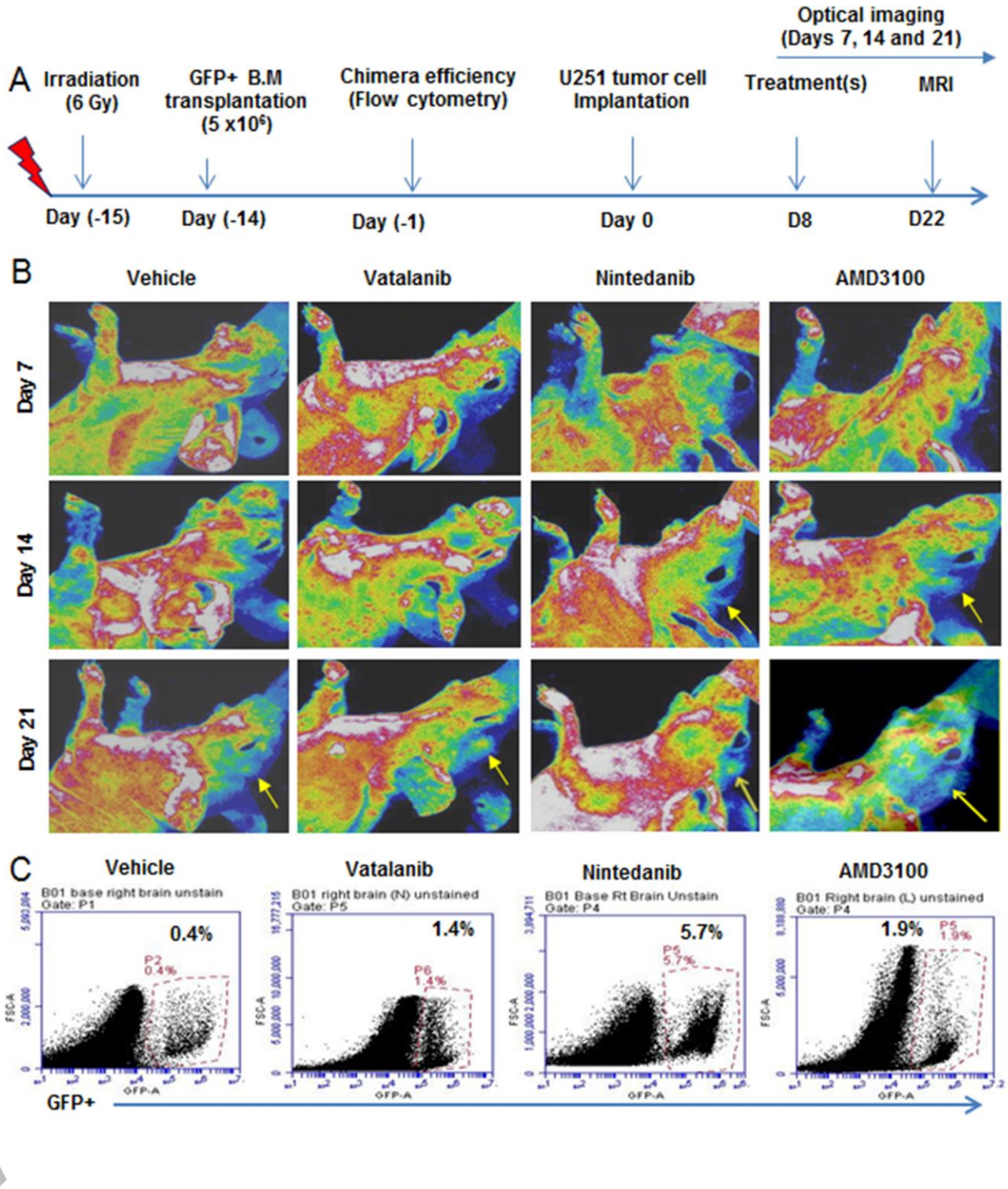

Figure 3: Effect of treatments on GFP+ cell infiltration to the tumor: (A) Schematic of chimera establishment, U251 tumor cells implantation, drug treatments and *in vivo* optical

imaging. **(B)** *In vivo* optical images obtained by Kodak In-Vivo Multispectral Imaging System FX (Carestream) on days 7, 14 and 21 showed increased accumulation of GFP+ in the tumor following treatments (yellow arrows) compared to vehicle, especially on day 21. GFP+ cells were detected in day14 tumors treated with nintedanib and AMD (yellow arrows). (**C**) Quantitative analysis by flow cytometry also proved the higher number of GFP+ cells in day 21 tumors that were treated with vatalanib, nintedanib and AMD3100.

Downloaded by [Georgia Regents University Greenblatt Library] at 07:07 22 January 2016

Accepted Manuscript

Downloaded by [Georgia Regents University Greenblatt Library] at 07:07 22 January 2016

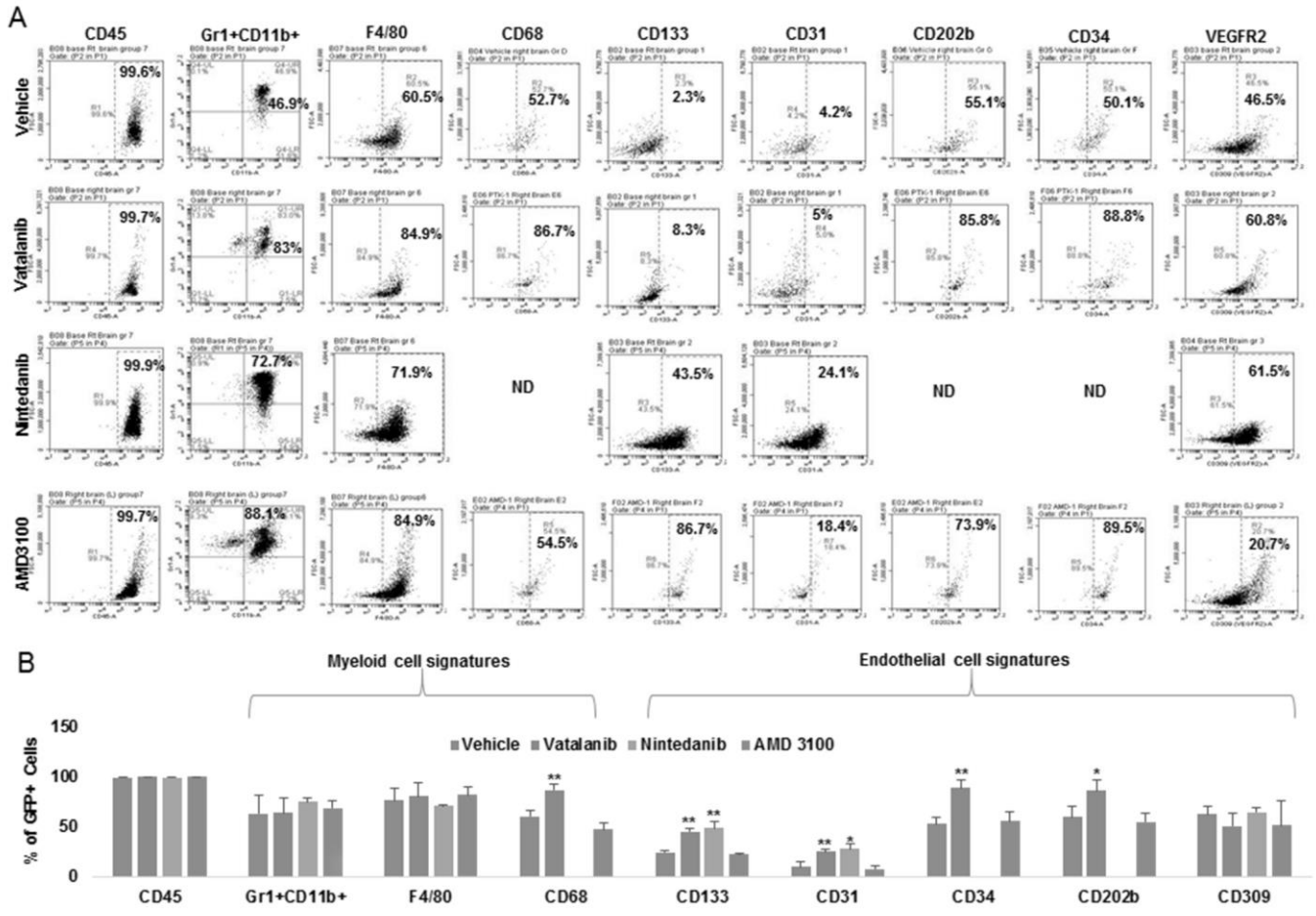

Figure 4. Effect of VEGFR2 kinase inhibitors and CXCR4 antagonist on myeloid and endothelial cell signatures in GBM tumor: Chimeric animals were implanted with orthotopic glioma (U251) and treated with vehicle, vatalanib, nintedanib, and AMD3100 from day 8-21. Tumor brains were collected after MRI and processed for flowcytometry analysis. **(A and B)** Vatalanib treatment significantly increased both myeloid signature (CD68) and endothelial signatures (CD133, CD31, CD202b, CD34) compared to vehicle (**A and B**). In addition, significant increase in endothelial cell signatures (CD133 and CD31) was seen in nintedanib group compared to vehicle (**A and B**). Please note we did not performt CD68, CD202b and

Accepted

CD34 stainings in nintedanib group (**A and B**). ND= not done. Quantitative data is expressed in mean ±SD. *P<0.05 and **P<0.01.

Downloaded by [Georgia Regents University Greenblatt Library] at 07:07 22 January 2016

Accepted Manuscript

Downloaded by [Georgia Regents University Greenblatt Library] at 07:07 22 January 2016

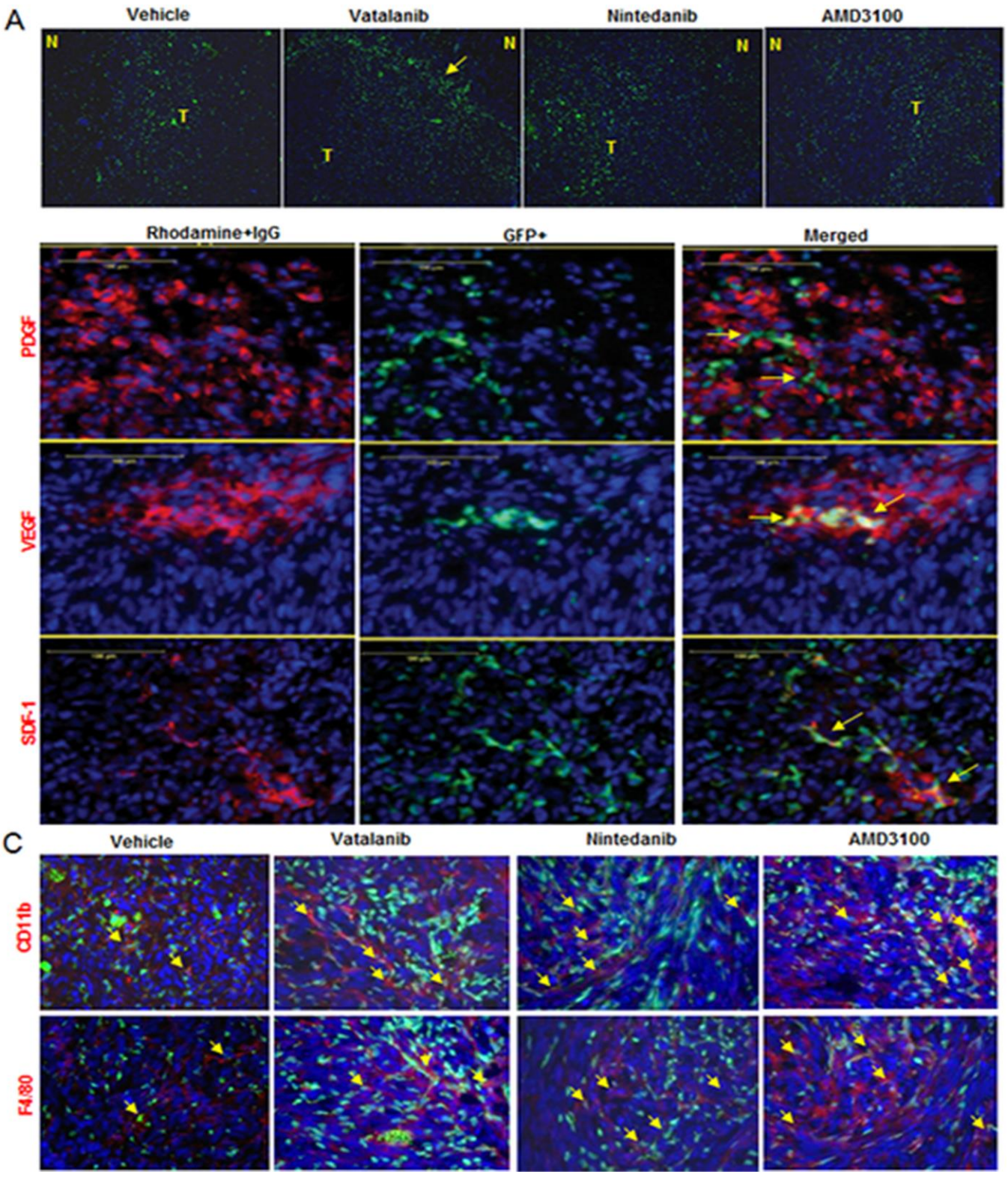

Figure 5. Accumulation of GFP+ cells in tumor and myeloid phenotypes. (A) Immunofluorescence images showing accumulation of GFP+ cells (green) at the tumor periphery or invasive front in vatalanib treated group (yellow arrow). (**B**) Co-localization of GFP+ cells with PDGF, SDF1 and VEGF expression (red) in the TME (yellow arrows). (**C**) Immunofluorescence images showing increased GFP+ cells (green) alongwith increased CD11b+ and F4/80+ cells (red) in vatalanib, nintedanib and AMD3100 treated groups compared to vehicle (yellow arrows). N= normal and T=tumor.

Downloaded by [Georgia Regents University Greenblatt Library] at 07:07 22 January 2016

Accepted Manuscript

View publication stats